Feasibility Study of the 3D Visualization at High Resolution of Intra-Cranial Rabbit Eyes With X-Ray CT Phase-Contrast Imaging

Yury Ivanishko,[1,2] Alberto Bravin,[3] Sergey Kovalev,[1,2] Polina Lisutina,[1,2] Mikhail Lotoshnikov,[1,2] Alberto Mittone,[3] Sergey Tkachev,[2] and Marina Tkacheva[1,2]

[1]Rostov Eye Clinic "InterYUNA", Rostov-on-Don, Russia
[2]Rostov State Medical University, Central Scientific Research Laboratory, Rostov-on-Don, Russia
[3]European Synchrotron Radiation Facility, ID17, Grenoble, France

Correspondence: Sergey Kovalev, Rostov Eye Clinic "InterYUNA", 148 Stachki Avenue, 344058 Rostov-on-Don, Russia; s.kovalev@list.ru.

Submitted: May 22, 2017
Accepted: October 23, 2017

Citation: Ivanishko Y, Bravin A, Kovalev S, et al. Feasibility study of the 3D visualization at high resolution of intra-cranial rabbit eyes with x-ray CT phase-contrast imaging. *Invest Ophthalmol Vis Sci*. 2017;58:5941–5948. DOI:10.1167/iovs.17-22273

Purpose. The intracranial three-dimensional (3D) visualization of the whole volume of the eyeball at micrometric resolution has not been achieved yet either in clinical nor in preclinical diagnostic research. Overcoming this limitation may provide a new tool for clinical and preclinical studies of different pathologies of the various sections of the eye. The aim of this work is to give the first insight of a volumetric visualization at the high resolution of the entire enucleated and intracranial postmortem rabbit eyeballs.

Methods. X-ray computed tomography phase-contrast imaging was used to obtain 3D models of enucleated and intracranial rabbit eyes. Images were compared with the ones measured by using optical coherence tomography (OCT) images. The experiment was carried out at the European Synchrotron Radiation Facility.

Results. Combining the unique possibilities offered by phase-contrast imaging, micro-tomography, and the properties of synchrotron radiation, the 3D visualization of the whole eyeball, at an isotropic voxel size of 3.1 μm^3, is reported here for the first time.

Conclusions. High image contrast is achieved without the necessity of injection of contrast agents, thanks to the superior performances, achieved by x-ray phase-contrast imaging with respect to the conventional radiographic imaging. The measurement protocol developed within this work opens the way for in vivo high-resolution visualization of the entire organ.

Keywords: ophthalmology, three-dimensional reconstruction, micro-tomography, x-ray phase-contrast imaging, propagation-based imaging

Preclinical and human diagnostic imaging methods used in ophthalmology include several complementary techniques like biomicroscopy; optical coherence tomography (OCT) and related confocal scanning laser ophthalmoscopy (cSLO); ultrasound scanning in the A- and B- mode (A- and B-scan); as well as ultrasound biomicroscopy (UBM); magnetic resonance imaging (MRI); and x-ray computed tomography (x-ray CT).[1] Histologic studies, which provide subcellular investigations, may be performed only postmortem; moreover, during the preparation of a histologic sample, tissues will be inevitably damaged by various factors, such as mechanical actions or chemical reagents so that histologic results are not always representative of the actual tissue architecture. Each clinical imaging method is particularly suitable to analyze a specific eye characteristic or to investigate the presence of a specific pathology; all methods also present specific requirements for their application. Both OCT and cSLO necessitate the transparency of the optical media to infrared laser scanning beams; these techniques are useful in studying a limited number of structures of the anterior segment of the eye and the fundus. The application of UBM is limited by the cornea and the anterior chamber angle. B-scan, conventional x-ray CT, and MRI allow visualizing the entire eyeball; but due to the limited resolution, these clinical methods do not provide a sufficient image quality and a detailed description of the anatomy. Therefore, outside oncology, they do not constitute a relevant diagnostic support in eye pathology. In recent years, micro-CT, performed postmortem in laboratories, allowed researchers to reach the resolution of 10 to 30 μm.[2] Micro-CT imaging always requires the use of contrast agents to enhance the very weak signal produced by soft tissues, which again leads to changes in tissue. The requirements for sample preparations for micro-CT[3] in general are complex, closely similar to procedures for histologic examinations and thus fundamentally unsuitable for in vivo application.

Since their discovery more than a century ago, as a radiation emitted by a Crookes' tube, x-rays have been applied to medical imaging and therapy. Until the appearance of dedicated synchrotron radiation (SR) sources in the late 70s and 80s, the x-ray sources have not much evolved in their general principle. The synchrotron x-ray sources became rapidly the golden standard, thanks to their exceptional characteristics in terms of wideness of the spectrum, of brightness, collimation, and ability to produce a coherent monochromatic beam, largely overpassing those of conventional x-ray tubes.[4] The unique properties of SR beams applied to biomedical imaging are fully exploited in phase-contrast imaging.[5] This class of techniques is sensitive to the phase shift occurring to x-rays passing through

TABLE. Today's Limiting Spatial Resolution of Various Imaging Techniques (μm)

				Laboratory		
MRI	B-scan	UBM	CT	Micro-CT	OCT	SR Micro-CT
250	150	30	100	10–30	4	1–5

an object rather than their attenuation. For light (low-Z) materials, like those composed of soft biologic tissues, the tissue differentiation made by the phase shift is much more sensitive than that made by attenuation, which is applied in conventional x-ray absorption imaging. This enhanced sensitivity allows the producing of images showing an unprecedented contrast, experimentally proven to be up to 100 times higher than that produced by the absorption properties of the same materials.

A possibility to overcome the diagnostic limitations of preclinical and clinical ophthalmology is offered by the application of phase-contrast imaging, which can provide a much higher spatial resolution (Table) at comparable or larger contrast levels than the most advanced implementations of the presently used intravital techniques, and without using any contrast agents.

Presently there are only two published works describing the application of SR for eye imaging use.[6,7] Kelly et al.[6] reported on the results of the study of formalin-fixed porcine eyes, using the analyzer-based imaging technique, and comparing them with the standard absorption images using the same parameters in terms of dose and x-ray energy. All images were acquired in radiographic mode, which suffers from structure overlap and does not allow for a high-resolution discrimination of the tissues. This was a seminal work, demonstrating the high potential of phase-contrast imaging in the study of the eye anatomy. Yin et al.[7] discussed the use of the same phase-contrast imaging technique, applied in the postmortem imaging of New Zealand rabbit eyes; the short paper does not report any detailed anatomic description of the findings.

In the present work, we propose for the first time full 3D ex vivo visualization with an isotropic voxel of ~3 μm of enucleated and intracranial rabbit eyes. The results here reported are obtained by using the propagation-based imaging technique without the need of contrast enhancer (contrast agents).

METHODS

Samples

Three healthy male European rabbits (Oryctolagus cuniculus, type HY107) were involved in the study (aged 16–20 weeks, average weight 2.5 ± 0.1 kg). Two kinds of samples were used for the SR experiment: enucleated eyes obtained postmortem from rabbits and full heads from the same species. Before the tissue extraction, animals were euthanized under deep anesthesia (5 L/min isoflurane + sodium pentobarbital 220 mg/kg). All applied animal protocols were carried out following the Article R-214-89 of the French Rural and Maritime Fisheries Code, the Directive 2010/63/EU of the European Parliament, and the ARVO Statement for the Use of Animals in Ophthalmic and Vision Research. The postmortem tissue extraction is classified as a "procedure without wake up." We would like to emphasize that samples did not undergo any pretreatment and no contrast agents were used for the imaging acquisition.

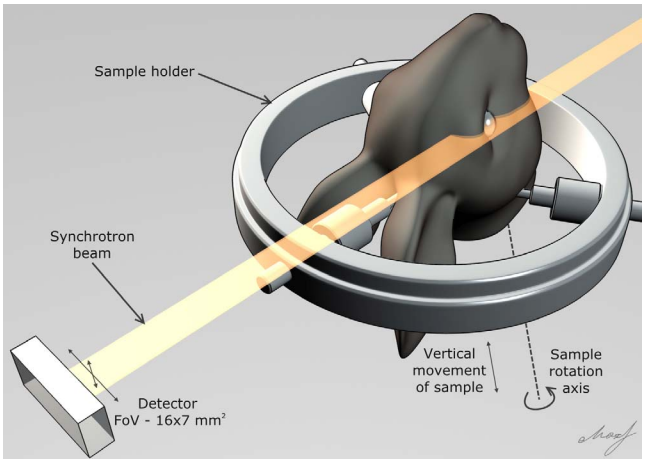

FIGURE 1. The sample positioning system and detector arrangement during the scanning a rabbit head.

For the purpose of the first part of the experiment, eyes were enucleated immediately after euthanizing and placed in a plastic cylinder containing a saline solution, which was then fixed on the rotation stage of the tomographic setup.

For the second part, the head—removed postmortem from the body—was then fixed vertically in a specially designed holder that allows for placement of the center of rotation inside the eyeball. With the specially designed holder, researchers could perform a CT while avoiding passage through the field of view and creating image artefacts (Fig. 1). As a validation step before potentially moving to in vivo imaging, the head position was chosen following two criteria: the beam path through the tissues outside the eye (bone, brain) had to be minimized and, at the same time, the position had to be physiologically compatible with respiration in in vivo experiments.

For comparison, we performed the OCT on two anesthetized healthy male European rabbits (Oryctolagus cuniculus) aged 20 weeks, average weight 2.6 ± 0.1 kg. Before examination, animals were sedated using an intramuscular administration of ketamine (10–20 mg/kg) and the pupils were dilated with a 1% cyclopentolate solution.

Phase-Contrast Imaging

Different phase-contrast techniques exist, which are characterized by different x-ray beam requirements and performances in terms of signal sensitivity. The most largely used are the propagation-based imaging,[8] the analyzer-based imaging,[9] the gratings interferometry,[10] and the edge illumination.[11] In the present study, we used the propagation-based imaging technique (PBI), which requires a highly coherent and quasi-monochromatic x-ray beam presently available only at SR facilities like the European Synchrotron Radiation Facility (ESRF) in Grenoble (France) where we performed our measurements. In PBI, the inhomogeneity inside of the sample induces a modulation of the x-ray wavefront and a consequent generation of diffraction patterns that can be recorded by a detector placed at a suitable distance from the sample.[8,12] The phase shifts are therefore transformed into detectable intensity variations as described by the Fresnel diffraction.[13] We have chosen this technique because it is particularly adapted to objects presenting multiple internal interfaces or showing internal structures like vascular or neuronal networks.[14] This method is widely used in preclinical radiology[5]; it allows users to obtain high-contrast images of soft tissues and, in

combination with CT, facilitates the building of 3D models of the studied object.

Phase-Contrast Images Acquisition and Image Processing

The experiments were performed at the biomedical beamline (ID17) of the ESRF. In order to apply the PBI technique, we used a quasimonochromatic ($\Delta E/E \sim 10^{-4}$), quasiparallel (divergence $\leq$ 1 mrad horizontally [H], and $<<$0.1 mrad, vertically [V]) x-ray beam. The monochromatic beam was selected from the continuous spectrum produced by the 21-pole wiggler source by a Si double Laue crystal monochromator system, which is tunable between 25 and 150 keV ($\lambda = 50$–8 pm).[15] The maximum beam footprint on the sample was 150 $\times$ 7 mm^2 (H $\times$ V). The propagation distance between the sample and the detector was set to 11 m. The tomographic scans were performed by rotating the sample in front of the beam and images (projections) were acquired at different angles. The detection system was a sCMOS PCO edge 5.5 camera (2560 $\times$ 2160 pixels) connected with a $\times$1:2 optics, holding a 350-µm thick, YAG-based scintillator screen to convert the x-rays into visible light. The imaging system pixel size was 3.1 $\times$ 3.1 µm^2; the detector field of view (FoV) was approximately 8.2 $\times$ 7 mm^2 (H $\times$ V). Using the half-acquisition CT modality, the finally available FoV was of approximately 16 $\times$ 7 mm^2. Due to the limited available vertical field of view, which was smaller than the sample, the volumetric image of the eye was obtained by displacing it vertically twice in between two CT acquisitions.

Images were acquired using a wide range of parameters in order to optimize the tissue visualization. This step was necessary because there was no literature in this field, which could have guided the setup of the imaging system. In the first part of the experiment, we acquired several datasets of the two types of samples (enucleated eyes or eye still in the orbit) at different beam energies: 30, 40, 50, 70 and 100 keV. The image analysis (see the Appendix section for an example) has indicated an optimized contrast at 50 keV in case of the enucleated eyes and at 70 keV for the full head imaging.

The number of the acquired angular projections varied between 500 and 4000. The acquisition was performed over 360° using the half acquisition mode, that allows to nearly double the available FoV.[16] The integration time for single projection was between 100 and 300 ms. The total acquisition time per sample ranged from few minutes up to 3 hours according to the experimental parameters. The whole head was imaged in local tomography condition because the size of the object was larger than the FOV. Artefacts related to the local tomography were removed by flattening the projection images background.

The reconstruction of the phase was performed using the quasiparticle phase-retrieval approach described in Moosmann et al.[17] The acquired images were reconstructed using the filtered-back projection algorithm[18] after the application of the single defocused-image Paganin algorithm[19] to extract the refraction signal.

For more technical information about image processing, see the Appendix section.

OCT Imaging

For comparison of our images with a reference diagnostic ophthalmology imaging method, we performed OCT because it is the only clinical method that permits the visualization of the retina at a comparable spatial resolution (Table) without inducing changes in the sample.

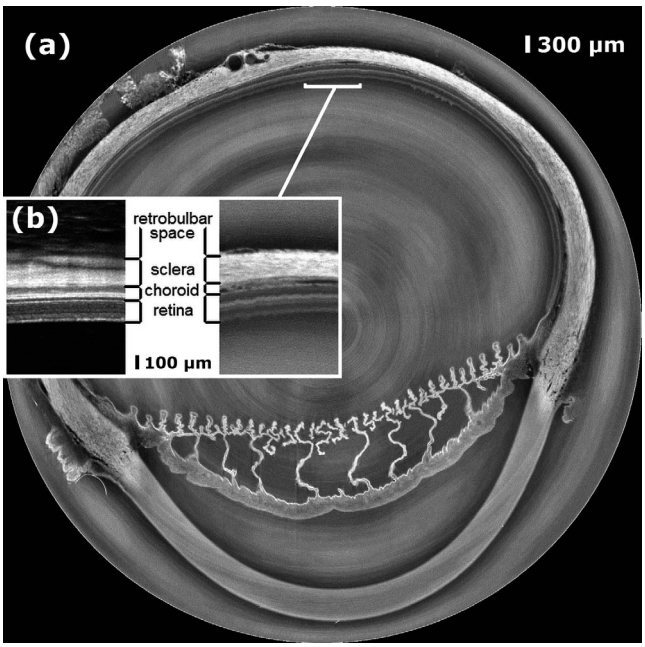

FIGURE 2. (**a**) CT slice of the enucleated rabbit eye (50 keV, 4000 projections). (**b**) Zoomed CT image (*right*) compared with the rabbit retina OCT (*left*) on the same scale (Optovue RTVue-100).

The OCT produces a real-time cross-sectional image of the neurosensory retina, retinal pigment epithelium, and choroid by using the interference between the reference optical path and the path reflected back from the eye.[20]

The OCT was performed using a commercial device (Optovue RTVue-100; Optovue, Inc., Fremont, CA, USA). The best images obtained were then chosen for the comparison with the phase contrast ones.

Dosimetry

We measured the dose delivered in the different experimental conditions used in the experiments following the protocol described in Mittone et al.[21] The air kinetic energy released per unit mass was measured using an ionization chamber, (0.125 cm^3 semiflex tube chamber, Model 31002; PTW-Freiburg, Freiburg im Breisgau, Germany) calibrated at the National Metrology Institute of Germany (Physikalisch-Technische Bundesanstalt, Braunschweig, Germany) and connected to the universal dosemeter module (UNIDOS; PTW-Freiburg). The dose distribution was then computed using Monte Carlo simulations as described in Mittone et al.[21] The model used in the simulations consisted of an elliptical shape of the dimensions of the rabbit head and the average dose was calculated in the region corresponding to the eye. The obtained values of doses vary according to the experimental parameters used during the acquisition within a range of 50 to 150 Gy.

RESULTS

The 3D rendering of the eye allows visualizing the smallest internal structure details due to the high contrast provided by the phase-contrast imaging method. Intracranial eye images are lower quality because of the larger number of artifacts caused by structural complexity and heterogeneous character of x-ray absorption of surrounding eye tissue (for a comparison, see the

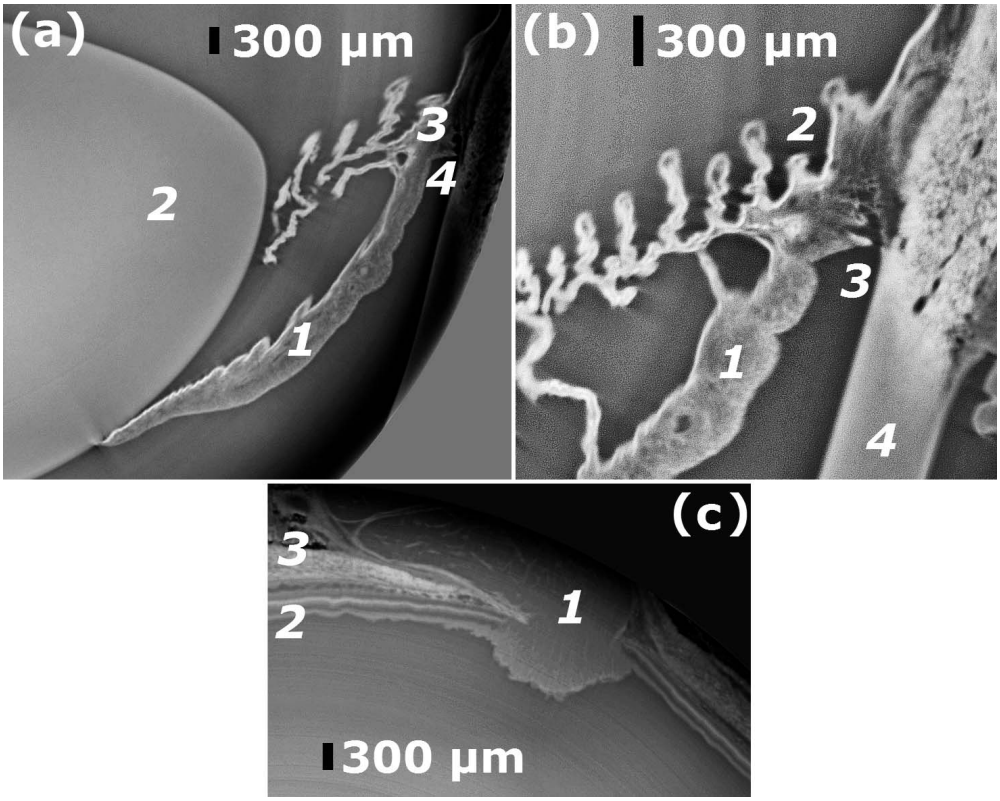

FIGURE 3. (**a**) CT slice of the enucleated rabbit eye (50 keV, 4000 projections): (1) iris, (2) lens, (3) ciliary body, (4) anterior chamber angle of isolated rabbit eye. (**b**) Magnified fragment of anterior chamber angle: (1) iris, (2) ciliary body, (3) trabecular meshwork, (4) cornea. (**c**) Posterior pole of the isolated rabbit eye: (1) optic nerve, (2) retina, (3) sclera.

Appendix section, Fig. A3). Separate 3D volume sections are shown in Figure 2.

Figure 2a is a cross-section of the enucleated rabbit eyeball in its upper part above the equator of the lens (therefore, the lens is not visible). The CT slice (3.1-µm thick) includes detailed profiles of the cornea, the sclera, the iris, the ciliary body, and the retina. Some layers of the retina were also visualized, which indicate that they possess different x-ray refraction properties.[5] The only clinical method, which allows visualizing the retina at a comparable spatial resolution, is the OCT. A portion of Figure 2a is magnified in Figure 2b (right) and compared with the OCT-image (left) of the rabbit retina on the same scale. Their similarities are undoubted, but the 3D volume composing the CT images is enormously richer because it can be reconstructed along any spatial direction (and not only retina as OCT 3D representation). Besides, it must be underlined that a detailed comparison between images obtained by PCI and OCT is intrinsically difficult because of the different nature of the probes (OCT: infrared light, PCI: hard X-rays) and of their interaction with the tissues.

Figure 3a shows the angle of the anterior chamber, the iris, the ciliary body, and the lens. Figure 3b is a magnified fragment of anterior chamber angle. Figure 3c shows instead of the posterior pole of the eyeball at the level of the optic nerve entering the sclera.

Figure 4 reports the 3D rendering of the intracranial eye imaging performed using the Amira data visualization software (Amira; Zuse Institut Berlin, Berlin, Germany).[22] Four different planes are reported in Figures 4a through 4d, respectively. Figures 4a and 4b show transverse sections. Figures 4c and 4d show frontal sections with the lens (in the center) and the ciliary body with the ciliary processes. The images present some remaining artefacts after the image processing (i.e., the transition between the different vertical frames and local differences in the image brightness); these artefacts originate from the presence of some dishomogeneities in the x-ray beam and the occurring of x-ray beam instabilities during the image acquisition.

DISCUSSION

Images of the rabbit eye in the skull require significantly more complex mathematical postprocessing than the enucleated eye because of the wider dynamic range of the images due to the presence of x-ray opaque bone structures surrounding the more radiotransparent eye tissues and because of several image reconstruction artefacts related to the local tomography condition. Despite all the named difficulties, we demonstrated the possibility of obtaining high-quality images of soft tissue structures in the surrounding bone of the skull and thus the interest in applying this technique in anesthetized live rabbits.

The long integration time required for the images is mainly ascribed to the extremely high spatial resolution applied to these images, which is at the cutting edge of the present technology to image an entire eye without the need to horizontally stitch images. In order to reduce the acquisition time (consequently, also the dose), we have margins both on the detection system and on reducing the number of acquired radiographs when combined with specific image reconstruction algorithms. The detection efficiency for the eye in the skull imaging can be improved by equipping the detector with a LuAG fluorescent screen instead of a YAG: at 70 keV, for the same thickness, the LuAG is four times more efficient. Low

Investigative Ophthalmology & Visual Science

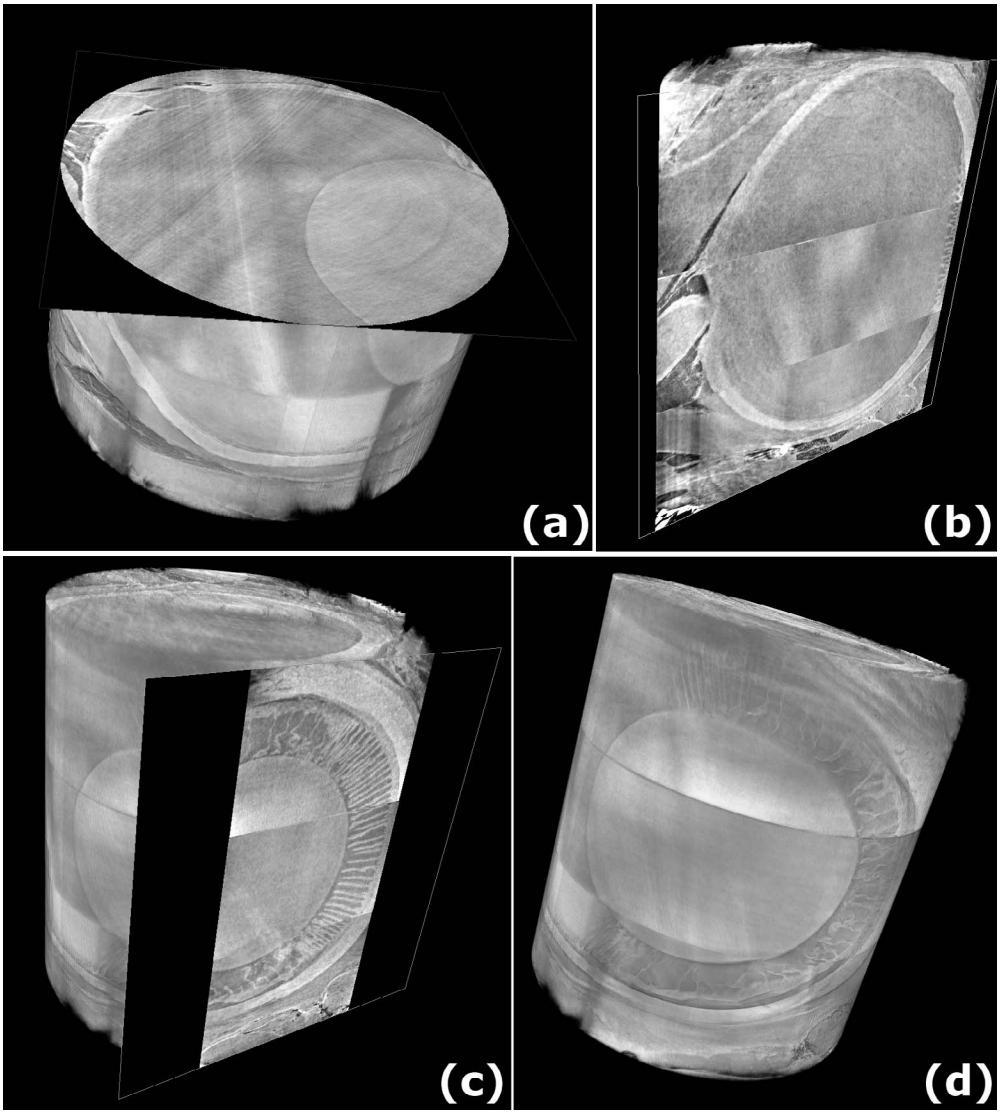

FIGURE 4. Examples of partial 3D reconstruction of intracranial rabbit eyes with sections in different planes. The external part with respect to the eye was removed. (**a**, **b**) Transversal view intersecting the optical nerve. (**c**, **d**) Frontal plane view with the lens, ciliary body, and ciliary processes.

statistic images could also be acquired and then processed using advanced reconstruction algorithms like the equally sloped tomography algorithm,[9] allowing reconstructions with a reduced number of angular projections. By implementing these technical improvements, the time and the x-ray doses needed to acquire the images might be reduced by a factor of 4 to 20.

A further reduction of the pixel size would be possible for the visualization of the enucleated eyes, for which both the imaging time and the dose are not an issue. It seems instead not feasible to use smaller pixel sizes in-view of the in vivo application of PCI: from one side, images will be even more prone to showing artefacts from the cardiosynchronous movements of the tissues, on the other one because of dose limitations: to obtain the same image quality (same statistics per pixel) the time and the dose increases with the inverse of the square of the pixel size.

By comparing the limiting values of spatial resolution of the imaging techniques used in ophthalmology,[20,23–25] it can be noted that the here-presented result is many times better than the majority of commonly used techniques and compete with the latest achievements in the field of optical coherence tomography of the retina. But if the OCT technique has now reached the limits in terms of spatial resolution due to the physical limitations imposed by the use of infrared light, and image quality can only evolve by the application of new improving mathematical methods,[20] the resolution of the images presented in this work can be even further increased by using higher resolution detectors. Furthermore, the phase-contrast imaging technique allows the visualization of all the intra- and periocular structures without limiting the researcher by retina only, and it enables the construction of 3D models of the surveyed structure without using any contrast agents.

The most important limitation of PCI is the fact that it requires a highly coherent x-ray beam presently available only at synchrotron radiation sources. The access to synchrotrons is very limited, due to their limited number in the world and because only a few of the 50 synchrotrons in the world are effectively equipped and suited to perform these kinds of studies. Due to these limitations, the potential clinical application of the methods proposed here will be possible only after the diffusion of the compact and relatively inexpensive sources presently under development around

the world.[26] In the meantime, our present main objective is to establish a platform for preclinical ophthalmologic research in vivo, for pathologies covering the entire eye bulb (and not only the eye but also other areas).

Conclusions

This proof of principle work shows the possibility of obtaining 3D images of ocular tissues and structures inside the animal head using hard x-rays. We have shown that this powerful method allows the visualization of the retina layers without requiring the use of contrast agents. The obtained results pave the way for carrying out similar studies in vivo in order to study dynamic processes.

Acknowledgments

The authors thank the European Synchrotron Radiation Facility (ESRF) for the provision of beam time through the proposal MD-1000, the ESRF-Biomedical Facility personnel for their support in the experiments.

Disclosure: **Y. Ivanishko**, None; **A. Bravin**, None; **S. Kovalev**, None; **P. Lisutina**, None; **M. Lotoshnikov**, None; **A. Mittone**, None; **S. Tkachev**, None; **M. Tkacheva**, None

References

1. Anastasio M, Riviere P. *Emerging Imaging Technologies in Medicine*. Boca Raton, FL: CRC Press; 2012.
2. Enders C, Braig E-M, Scherer K, et al. Advanced non-destructive ocular visualization methods by improved x-ray imaging techniques. *PLoS One*. 2017;12:e0170633.
3. de Souza e Silva JM, Zanette I, Noel PB, Cardoso MB, Kimm MA, Pfeiffer F. Three-dimensional non-destructive soft-tissue visualization with x-ray staining micro-tomography. *Sci Rep*. 2015;5:14088.
4. Suortti P, Thomlinson W. Medical applications of synchrotron radiation. *Phys Med Biol*. 2003;48:R1–R35.
5. Bravin A, Coan P, Suortti P. X-ray phase-contrast imaging: from pre-clinical applications towards clinics. *Phys Med Biol*. 2013; 58:R1–R35.
6. Kelly ME, Coupal DJ, Beavis RC, et al. Diffraction-enhanced imaging of a porcine eye. *Can J Ophthalmol*. 2007;42:731–733.
7. Yin HX, Huang ZF, Wang ZC, Liu ZH, Li Y, Zhu PP. Application research of DEI technique based on synchrotron X-ray source in imaging rabbit eyeball in vitro. *Zhonghua Yi Xue Za Zhi*. 2010;90:777–781.
8. Snigirev A, Snigireva I, Kohn V, et al. On the possibilities of X-ray phase contrast microimaging by coherent high-energy synchrotron radiation. *Rev Sci Instrum*. 1995;66:5486–5492.
9. Zhao Y, Brun E, Coan P, et al. High-resolution, low-dose phase contrast X-ray tomography for 3D diagnosis of human breast cancers. *Proc Natl Acad Sci U S A*. 2012;109:18290–18294.
10. Pfeiffer F, Weitkamp T, Bunk O, et al. Phase retrieval and differential phase-contrast imaging with low-brilliance X-ray sources. *Nature Phys*. 2006;2:258–261.
11. Olivo A, Arfelli F, Cantatore G, et al. An innovative digital imaging set-up allowing a low-dose approach to phase contrast applications in the medical field. *Med Phys*. 2001; 28:1610–1619.
12. Cloetens P, Barrett R, Baruchel J, Guigay JP, Schlenker M. Phase objects in synchrotron radiation hard X-ray imaging. *J Phys D Appl Phys*. 1996;29:133–146.
13. Born M, Wolf E. *Principles of Optics: Electromagnetic Theory of Propagation, Interference and Diffraction of Light*. 7th ed. Cambridge: Cambridge University Press; 1999.
14. Bukreeva I, Campi G, Fratini M, et al. Quantitative 3D investigation of neuronal network in mouse spinal cord model. *Sci Rep*. 2017;7:41054.
15. Suortti P, Fiedler S, Bravin A, et al. Fixed-exit monochromator for computed tomography with synchrotron radiation at energies 18-90 keV. *J Synchrotron Radiat*. 2000;7:340–347.
16. Zamir O, Arthurs C, Hagen P, et al. X-ray phase contrast tomography; proof of principle for post-mortem imaging. *Br J Radiol*. 2015;89:20150565.
17. Moosmann J, Hofmann R, Baumbach T. Single-distance phase retrieval at large phase shift. *Opt Express*. 2011;19:12066–12073.
18. Kak AC, Slaney M. *Principles of Computerized Tomographic Imaging*. New York, NY: IEEE Press; 1988.
19. Paganin D, Mayo SC, Gureyev TE, Miller PR, Wilkins SW. Simultaneous phase and amplitude extraction from a single defocused image of a homogeneous object. *J Microsc*. 2002; 206(part 1):33–40.
20. Zawadzki RJ, Cense B, Zhang Y, Choi SS, Miller DT, Werner JS. Ultrahigh-resolution optical coherence tomography with monochromatic and chromatic aberration correction. *Opt Express*. 2008;16:8126–8143.
21. Mittone A, Baldacci F, Bravin A, et al. An efficient numerical tool for dose deposition prediction applied to synchrotron medical imaging and radiation therapy. *J Synch Rad*. 2013; 20(Pt 5):785–792.
22. Stalling D, Westerhoff M, Hege HC. *Amira: A Highly Interactive System for Visual Data Analysis. The Visualization Handbook*. Burlington, MA: Elsevier; 2005:749–767.
23. Ritman EL. Medical x-ray imaging, current status and some future challenges. *Advances in X-Ray Analysis*. 2006;49:1–12. Available at: http://www.icdd.com/resources/axa/vol49/v49_01.pdf.
24. Silverman RH. High-resolution ultrasound imaging of the eye – a review. *Clin Exp Ophthalmol*. 2009;37:54–67.
25. Van Wijk DF, Strang AC, Duivenvoorden R, et al. Increasing spatial resolution of 3T MRI scanning improves reproducibility of carotid arterial wall dimension measurements. *MAGMA*. 2014;27:219–226.
26. Jacquet M, Suortti P. Radiation therapy at compact Compton sources. *Phys Med*. 2015;31:596–600.
27. Chambolle A. An algorithm for total variation minimization and applications. *J Math Imaging Vis*. 2004;20:89–97.

Investigative Ophthalmology & Visual Science

Appendix

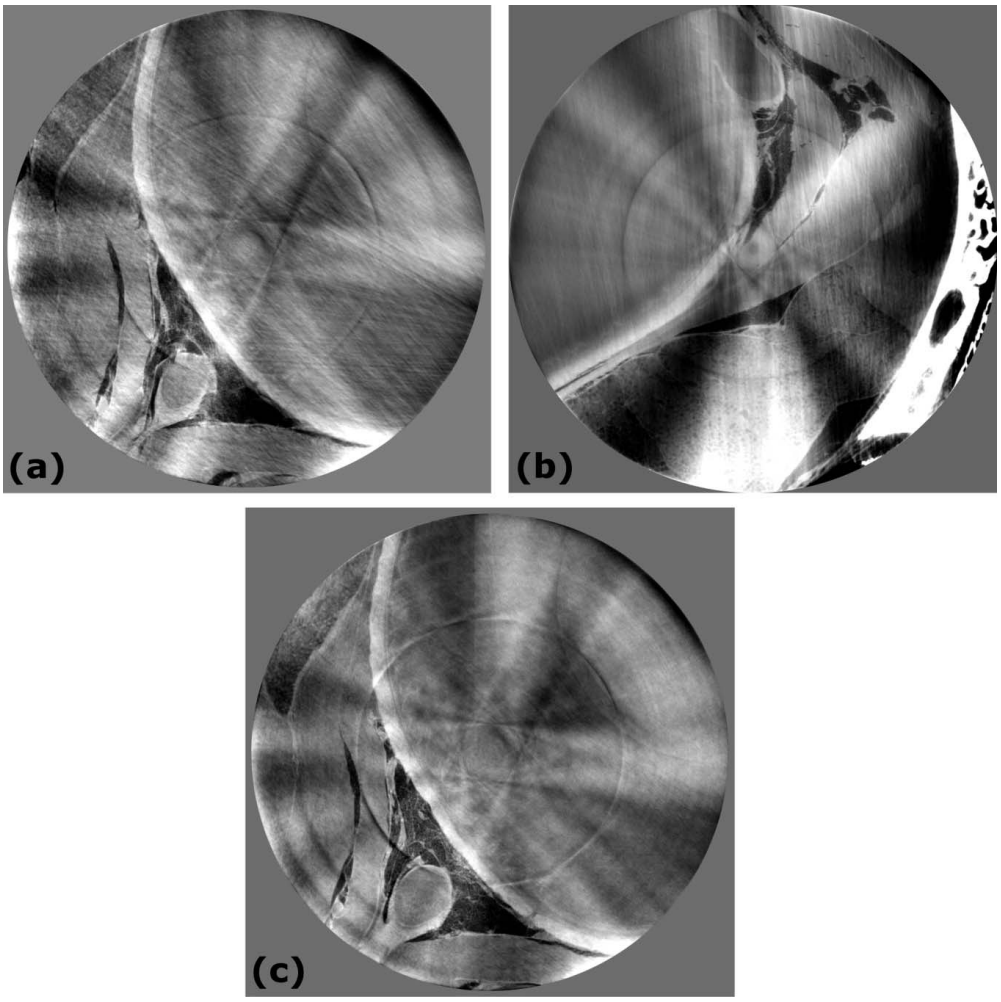

Figure A1. Different intracranial sections acquired at different x-ray energies. In all three images, it is possible to identify the optic nerve: (**a**, **c**) *bottom left*, (**b**) top center; (**a**) and (**c**) are from the same section of the sample. Image acquired at (**a**) 50 keV, (**b**) 70 keV, and (**c**) 100 keV. The data presented here have been used as a test for the online optimization. Therefore, very little image processing has been applied to remove the various artefacts. Following the results of this study, the 70 keV case has been selected for the successive measurements. This energy represents a good compromise in terms of contrast and transmitted signal and fits well with the characteristics of the monochromator used at ID17, optimized for 80 keV. In comparison to (**a**) and (**c**), (**b**) on average presents more artefacts due to the presence of bone tissue on the right side.

Investigative Ophthalmology & Visual Science

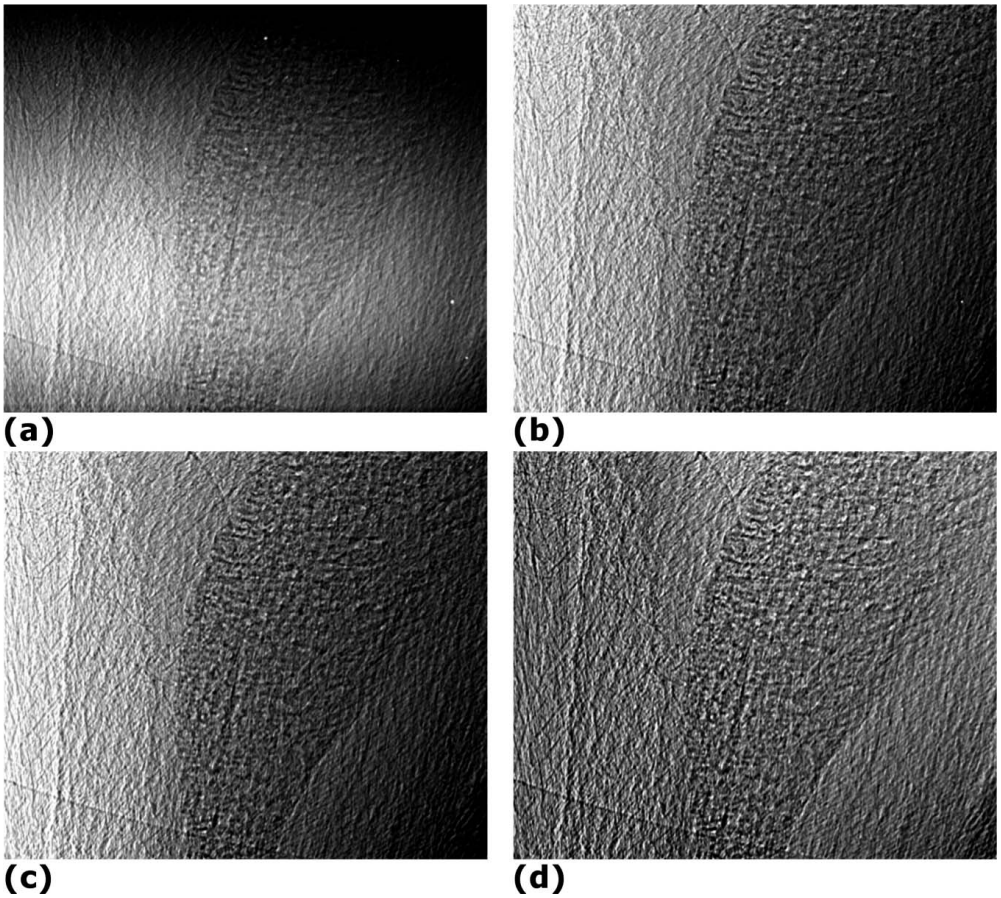

FIGURE A2. Image preprocessing chain. (**a**) Original projection acquired. (**b**) Projection after normalization on its reference. (**c**) Projection after removal of hot spots linked to defect on the scintillator screen. (**d**) Final results after removal of the image background using the total variation method.[27] For the image processing, an ad-hoc code has been written in Python. Several methods and procedures have been implemented to process the original projections in a multi-step approach. The major processing steps are reported in the Figure. Different methods have been tested before to optimize the results.

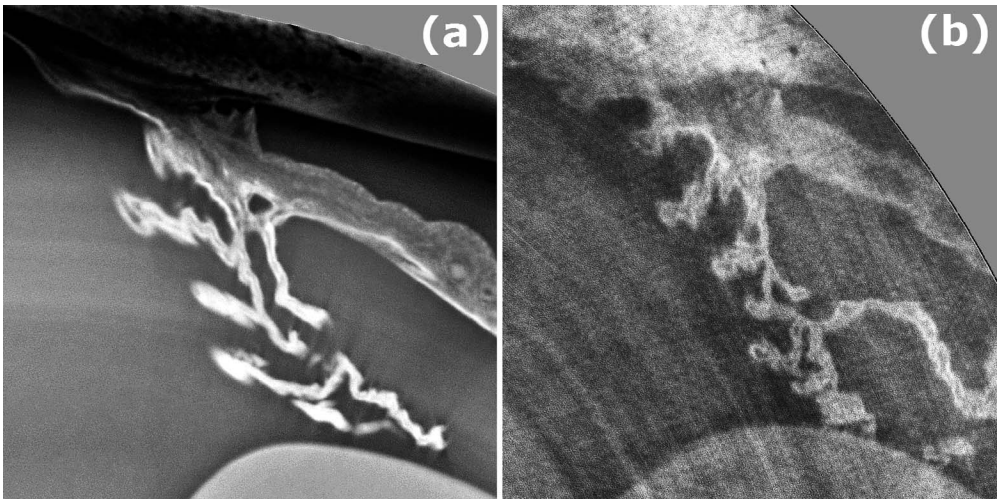

FIGURE A3. Comparison of the same zone (anterior chamber angle) of (**a**) isolated and (**b**) intracranial rabbit eye.

Investigative Ophthalmology & Visual Science